Clinical Oncology (2004) **16**: 307–316
doi:10.1016/j.clon.2004.01.013

Original Article

Determination of Tumour Prognosis Based on Angiogenesis-related Vascular Patterns Measured by Fractal and Syntactic Structure Analysis

B. Weyn†§, W. A. A. Tjalma†, P. Vermeylen‡, A. van Daele†#, E. Van Marck‡, W. Jacob*

†Center for Electron Microscopy, University Hospital Antwerp (UIA), Antwerp, Belgium; ‡Department of Gynecology and Gynecologic Oncology, University Hospital Antwerp (UIA), Antwerp, Belgium; #Laboratory of Pathology, University of Antwerp (UIA), Antwerp, Belgium; §Digital Cell Imaging Labs, Edegem, Belgium

ABSTRACT:
Aims: Intratumoural micro-vessel density (IMD) has recently been shown to be a valuable prognostic tool in many tumours. Yet, IMD does not take into account the spatial arrangement of the vessels, therefore only partly reflecting the angiogenic situation. In order to describe contextual vascular relationships more accurately, we have used fractal and syntactic structure analysis (SSA) based on computerised image processing to quantify micro-vascular hot spots.
Materials and methods: The parametric performance in prediction of patients' outcome was evaluated by univariate analysis and compared with manually obtained IMDs, whereas an automated K-nearest-neighbour (KNN) classifier searched most discriminative parametric combinations. The method is based on analysis of vascular 'hot-spots' of paraffin-embedded tissue sections of invasive cervical carcinoma, colorectal carcinoma and malignant mesothelioma.
Results: For all three cancers, prediction of prognosis based on SSA yielded in general much higher recognition scores compared with IMD or fractal dimension. Survival of cervical carcinoma was mostly correlated with clinical data, with the vascular permeation being the only parameter with independent value. Prognosis of colorectal carcinoma is best described by SSA, completed with IMD, indicating an inverse correlation of survival time with a more irregular pattern and a slight increase in vessel number. For mesothelioma, we found a strong correlation with SSA and patients' outcome, with two SSA-parameters having independent prognostic value.
Conclusions: The more accurate angiogenic description obtained with SSA may be useful for further exploitation as a prognosticator in a general diagnostic pathology service. Weyn B. *et al.* (2004). *Clinical Oncology* **16,** 307–316

Key words: Syntactic structure analysis, angiogenesis, fractal analysis, quantitative pathology, prognosis, cancer

Received: 1 October 2003 Revised: 22 January 2004 Accepted: 27 January 2004

Introduction

Neo-angiogenesis, the formation of blood vessels in tumours, is an interactive process between tumour, endothelial and stromal cells in order to create a network supplying oxygen and nutrients necessary for tumour growth. The blood vessels can also spill tumour cells throughout the host, associating angiogenesis directly with the formation of metastases [1,2]. Given this critical role in tumour enlargement and metastatic potential, it is not surprising that prognosis is directly related to the degree of intratumoural vascularisation in many tumours [3–18].

Author for correspondence: Wiebren A. A. Tjalma, MD PhD Professor, University Antwerp, Department of Gynecology and Gynecological Oncology, University Hospital Antwerp, Wilrijkstraat 10, 2650 Edegem, Belgium. Tel: ++ 32 3 821 59 04; Fax: ++ 32 3 825 58 83; E-mail: wiebren.tjalma@uza.be

The angiogenic potential is usually estimated by manually counting the number of blood vessels in a vascular 'hot-spot' of an anti-endothelium immunostained section, and expressed per unit of area as 'intratumoural micro-vascular density' (IMD) [19–21]. However, inter-observer variability and extensive observation have encouraged the use of image analysis. This method consists of scanning the tumoural section manually for vascular 'hot-spots' and taking images at a larger magnification from these regions. An automated procedure is then started, resulting in the calculation of vessel-derived parameters with prognostic potential, such as vessel area, intervascular distance or luminal area. Several reports show that these parameters often have a stronger prognostic correlation than the IMD, which may indicate that the use of image analysis in the assessment of angiogenesis can increase the accuracy and prediction of prognosis [19–23].

0936-6555/04/040307+10 $30.00/0

In this respect, it may be interesting to evaluate the prognostic potential of the contextual relationship between the capillaries, which has, as far as we know, never been studied. The formation of new blood vessel starts with the triggering of an existing mature blood vessel by angiogenic factors derived from tumour and activated stromal cells after which the vascular basement membrane is degraded. Endothelial cells then migrate in the direction of the angiogenic stimuli and start to proliferate. After formation of a lumen, the tips of individual sprouts join together to form capillary loops [24,25]. On the basis of this theory, one can presume that the position of the newly formed vessels is dependent upon the stromal histology, the position of blood vessels adjacent to the tumour and the local concentration and type of angiogenic factors. These comprise the transformed tumour-cell phenotype and the reciprocal tumour-host interactions, and reflect directly the prognosis of the individual patient. Moreover, comparison of contextual data from vascular patterns may give insight into angiogenic development during transformation, and may contribute to the understanding of the multistep-angiogenic process.

In this paper, we have tried to evaluate the prognostic power of neovascular arrangements by two different approaches. First, we have calculated the fractal dimension of micro-vascular 'hot-spots' in order to describe the homogeneity and irregularity of the patterns [26–28]. Fractal analysis is only sparsely applied in angiogenic quantification, although its potential is striking [29,30]. The energetic principle for least energy cost for blood flow is compatible with the spatial constraints of arterial networks according to concepts derived from fractal geometry [31]. Fractal dimensions give information about both the regularity of the individual vessels and the positioning of the vessels inside the tumour, and, therefore, comprise several levels of spatial angiogenic organisation [32]. Second, the arrangement of vascular spatial positions was quantified with syntactic structure analysis (SSA), a method often used for quantification of tissue architecture [33,34]. This approach uses a binary representation of the centres of gravity of individual vessels to construct graphs or diagrams of which the characteristics are applied as contextual parameters [35]. Examples of such figures are the Voronoi diagram, the Gabriel's graph and the minimum spanning tree, which may give insight into the division of the blood supply inside the tumour and the immediate and distant vascular neighbourhood relationships, respectively.

Both techniques were evaluated on CD31-immunostained sections of three different tumours (i.e. malignant mesothelioma, invasive cervical carcinoma and colorectal carcinoma). Angiogenesis and its prognostic potential are described in detail for the three lesions, which provides data that can be used to compare with our results [36–43]. Besides the aforementioned parameters, we have also calculated the more 'classical parameters' like IMD, vessel area, lumen and perimeter, which were used together with some clinical data, as 'internal references'. The prognostic value of all parameters was estimated by classifying the samples according to survival time with the aid of a K-nearest-neighbour (KNN) classifier coupled to Fast Forward Feature Selection. The method presents the best discriminative combination of parameters by searching the highest possible recognition score. It provides information on the individual performance of the parameters as well as complementary information on the diverse vascular aspects.

Materials and Methods

Patients and Follow-up

All blocks were obtained from the archives of the University Hospital Antwerp and the General Hospital Saint Camillus-Saint-Augustinus, Belgium. The selection criterion was a tissue size of at least 5×5 mm, preferably including the tumour border. Survival times were measured from time of diagnosis.

For cervical carcinoma, the histological diagnosis, tumour grade, lympho-vascular space invasion and lymph-node status were determined during routine pathological assessment. Histological classification was based on World Health Organization criteria. A total of 61 patients with squamous cell carcinoma, 10 patients with adenocarcinoma and seven patients with adenosquamous carcinoma were studied. The mean age of the patients was 48.9 years. Nineteen cases showed grade I tumour differentiation, 27 cases grade II and 32 cases grade III. Fifteen per cent of the cases was FIGO staged 0, 18% Ia, 32% Ib, 17% IIa, 6% IIb, to IIIa and IIIb and 1% IVa. The lower stages (0–IIa) were treated by surgery, and radiotherapy was added if the lymph nodes were positive. The higher stages (IIB–IV) were mainly treated by radiotherapy with or without concomitant chemotherapy. The median follow-up time was 34 months (range 4–117 months).

For colorectal carcinoma, we studied 74 full-cross sections of colorectal adenocarcinoma surrounded by colorectal mucosa. The mean age of the patients was 64.3 years and the median follow-up period was 33.0 months (range 1.9–75.1 months). One tumour was classified as Duke's A, 24 tumours as Duke's B, 37 as Duke's C and 12 as Duke's D. Thirty-eight per cent were graded in class I, 53% in class II and 7% in class III. Twenty-eight of the tumours were well-differentiated, 39 moderately and seven poorly. All patients without distant metastasis were treated by surgery. Duke's C patients received adjuvant chemotherapy. Duke's D patients were treated by palliative chemotherapy.

For malignant mesothelioma, we studied 27 cases, of which 13 were epithelial, five sarcomatous and nine biphasic. Thirty-five per cent of the tumours were staged as stage I, 40% as stage II and 25% as stage III. Thirty-three per cent had grade I, 39% grade II and 28% grade III. The mean age for this group was 62.4 years, with an average survival of 11.5 months (range

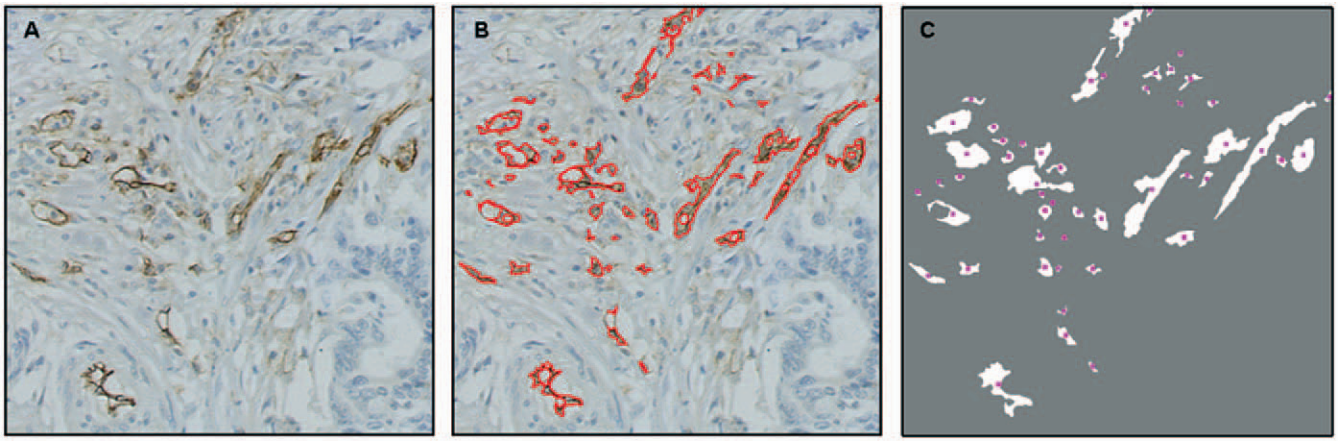

Fig. 1 – (a) Digitised image of a vascular 'hot-spot' of a colorectal carcinoma; (b) contours of the resulting binary image after thresholding–thresholding of the original colour image; (c) vascular centres of gravity (dots) and their associated vessels on which the syntactic structure analysis are based.

0.01–86.2 months). All patients were treated with surgery in combination with (palliative) radiotherapy or chemotherapy.

Immunohistochemistry

Five-micrometer thick sections were placed on 3-aminopropyltriethoxysilane (Sigma, UK) coated glass slides, and treated with 0.3% hydrogen peroxidase in methanol to block endogenous peroxidase activity for 30 min. Antigen-retrieval was carried out by immersion of the slides in trypsin (1 mg/ml) in phosphate-buffered saline (BPS) for 10 min at 37°C, and heating in a microwave oven at 95°C for 15 min. After cooling at room temperature for 1 h, the slides were incubated with the anti-CD31 monoclonal antibody JC 70 (Dako, Glostrup, Denmark) and diluted 1/40 for 90 min in PBS containing 1% bovine serum albumin (Sigma, UK). After three washes with PBS, the slides were incubated with biotinylated rabbit anti-mouse antibodies for 30 min (Dako, dilution 1/200). Visualisation of the immunocomplex was done by using a standard avidin-peroxidase conjugated biotin technique using diaminobenzidine as the chromogen, followed by a haematoxylin counter-stain for a few seconds.

Digital Image Analysis and Quantification of Tumour Vascularity

All the measurements were carried out with a VIDAS-25 digital image analysis system (Kontron, Munich, Germany) coupled to a 3-chip colour CCD camera (JVC, Yokohama, Japan) placed on the phototube of an Axiolab Zeiss microscope (Oberkochen, Germany). The entire tumour section was systematically scanned with a 10× objective to identify the areas with most intense neo-vascularisation [44]. Whenever a highly vascularised area was found, the objective was changed to a 20× lens, and 24-bit 512^2-colour images were taken randomly in the hot spot. Depending on the hot-spot size, 2–10 fields were taken per sample. These images were corrected for background illumination using standard VIDAS-software and segmented based on differences with the aid of a house-written macro (Fig. 1). The resulting contours of the immunostained areas were displayed in the original colour image and, whenever erroneous segmentation was encountered, corrected by a supervisor. For each image, the following vessel-related parameters were measured: IMD, total vessel perimeter, total endothelial-stained area and mean vessel area. In addition, the amount of single micro-vessels was counted manually in each image as any brown-stained area. Occasional immunopositive macrophages and plasma cells were excluded on morphological grounds. These parameters were completed with SSA and fractal parameters (Table 1).

Syntactic Structure Analysis

The centres of gravity of the vessels were replaced by labelled pixels that were used to construct three different figures: the Voronoi diagram, the Gabriel's graph and the minimum spanning tree (Fig. 2).

The Voronoi diagram divides the image plane into a lattice of adjacent polygons where each core has an associated vascular centre of gravity in a way that every point inside the polygon is closer to that core than to any other core in the image. This reveals the 'zone of influence' of each vessel, and may give an idea about the distribution of the blood supply inside the tumour. Note that this blood supply is highly dependent on blood-flow-rate within the individual vessels, which is notoriously heterogeneous. To minimise edge effects, the Voronoi polygons located at the border of the

Table 1 – Overview of descriptors used in this study. Parameters are used as a mean and standard deviation of the population

Group	Name	Definition
Fractal analysis	FD	Fractal dimension vascular pattern
	M_FD, G_FD	Fractal dimension GG, MST
Vessel-derived	VES_CNT	Vessel count (quantitative)
	MAN_CNT	Vessel count (manual)
	PAPAREA	Immunostained area (with lumen)
	VES_AREA	Vessel area (without lumen)
	VES_PERIM	Vessel perimeter
SSA	G1, M1	Total length of GG (MST)/unit reference area
	G2, M2	Number of branches of GG (MST)/unit reference area
	G3, M3	Mean length of branches of GG (MST)
	G4, M4	SD of length of branches of GG (MST)
	G5, M5	Skewness of length of branches of GG (MST)
	G6, M6	Kurtosis of length of branches of GG (MST)
	G7, M7	Mean number of branches/node of GG (MST)
	G8, M8	SD of number of branches/node of GG (MST)
	G9, M9	Skewness of number of branches/node of GG (MST)
	G10, M10	Kurtosis of number of branches/node of GG (MST)
	G11, M11	Mean distance to the nearest neighbours of GG (MST)
	G12, M12	SD of distance to the nearest neighbours of GG (MST)
	G13, M13	Skewness of distance to the nearest neighbours of GG (MST)
	G14, M14	Kurtosis of distance to the nearest neighbours of GG (MST)
	V1	Total number of vessels/reference area
	V2	Mean area of Voronoi's
	V3	SD of area of Voronoi's
	V4	Skewness of area of Voronoi's
	V5	Kurtosis of area of Voronoi's
	V6	Mean of shapes of Voronoi's
	V7	SD of shapes of Voronoi's
	V8	Skewness of shapes of Voronoi's
	V9	Kurtosis of shapes of Voronoi's
	V10	Mean of forms of Voronoi's
	V11	SD of forms of Voronoi's
	V12	Skewness of forms of Voronoi's
	V13	Kurtosis of forms of Voronoi's
Clinical Data	age	Age at diagnosis
	VASCPERM	Vascular permeation
	LYMPHERM	Lymphatic permeation
	LN_META	Lymphatic metastasis

GG, Gabriel's Graph; MTS, Minimum Spanning Tree; SD, standard deviation.

sampling window were excluded from the measurements. Parameters derived from this graph are (1) the area of the polygons; (2) the polygonal form (defined as the area multiplied by 4 and divided by the quadrate of the perimeter); and (3) the polygonal shape (defined as the ratio of the minimal and maximal diameter).

The Gabriel's graph is composed of line segments connecting two vascular centres of gravity, which are drawn when they cross the border of adjacent Voronoi polygons exactly one time. The figure completes in this way the information of the Voronoi diagram, and gives insight into the immediate neighbourhood arrangements of the vessels. From this graph, we calculated (1) total length per reference area; (2), number of branches per reference area; (3) mean length of the branches; (4) number of branches or node; (5) mean distance to the nearest adjacent neighbours; and (6) fractal dimension.

The minimum spanning tree is composed of line segments connecting two vascular centres of gravity in a way that the total length of the graph is minimal and that no loops are formed. The characteristics relate to the overall positioning of the vessels in the hot spot but give also information about the immediate relationships between the vessels. Parameters are similar as those used in quantifying the Gabriel's graph.

For all three figures, and for all parameters, the mean, standard deviation, skewness and kurtosis were calculated for each field.

Fractal Analysis

The fractal dimension, in this paper assessed by the box-counting method, indicates the plane-filling capacity in a sense that highly irregular figures with a large degree of self-similarity will give a higher value [45–48]. To calculate the fractal dimension, we divided the image into squares with size 'e', and counted the amount of squares (or boxes) that contain at least 1 pixel belonging to a vascular feature (N [e]). N (e) is then averaged by shifting the grid-lattice several times within the plane. This procedure is repeated with increasing

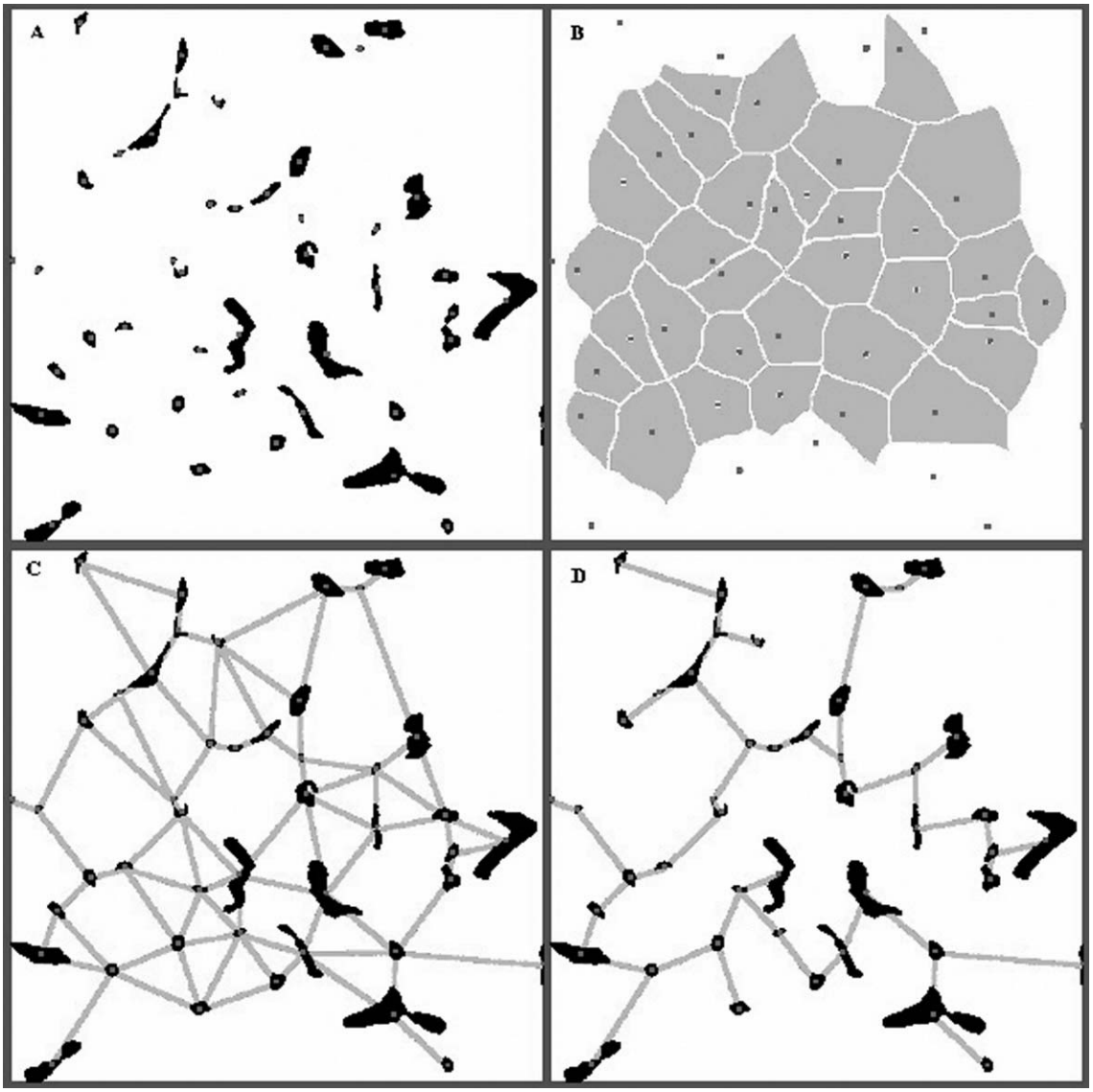

Fig. 2 – Voronoi diagram (b), Gabriel's graph (c) and minimum spanning tree (d) of binary image (a). The black areas represent the vessels; the dots their centres of gravity, and the light gray lines or polygons the syntactic figures.

box-size, and the counts are plotted against the size of the boxes in a logarithmic diagram (log N [e] vs log [e] graph). Between the limits of self-similarity, the graph shows a straight line, of which the negative value of the slope is defined as 'fractal dimension'. Fractal analysis was applied on the binary images containing the immunostained areas and on Gabriel's graph and minimum spanning tree figures with line segments of 1 pixel thick.

Sample Classification

K-nearest-neighbour classification

Multivariate sample classification was performed using the KNN-classifier because of its versatile and user-friendly characteristics [49]. This classifier can be seen as an N-dimensional representation space, in which each axis represents the magnitude of a single parameter. The elements of the space are single points, each representing a tumour case, of which the position is defined by the magnitude of the describing parameters. Similar cases will be defined by similar parametric magnitudes, and will therefore form clusters. The idea of the classifier is to define the edges of these clusters by positioning labelled points (i.e. from a predefined type) in the space. This is called the training phase. The value of the classifier is estimated by positioning non-labelled cases of a test set of a known type in this space and labelling them similarly as the K-nearest neighbours. The assigned label is then compared with the true label

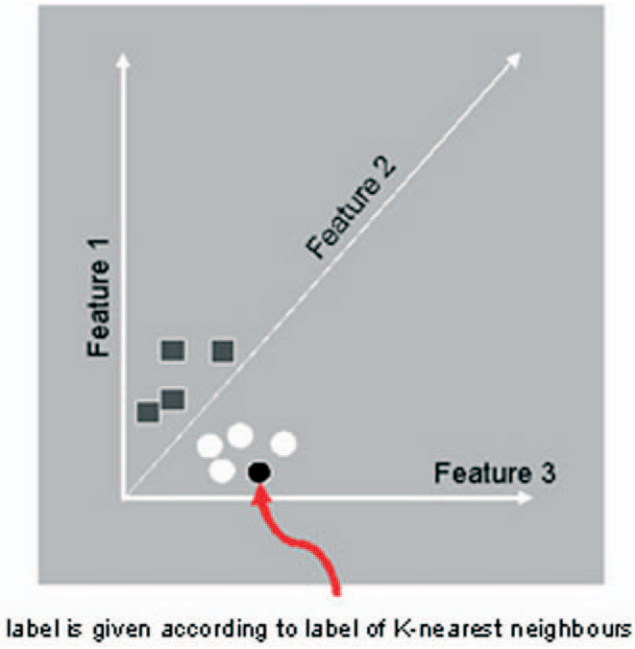

Fig. 3 – The K-nearest-neighbour classifier.

and expressed as the percentage of correctly labelled cases or the 'recognition score'. Concerning the choice for K, only limited theoretical results are available [30]. Therefore, we have determined K experimentally and the 1 nn classifier (K=1) proved to yield the best results. The major drawback of the classifier is the deterioration of the performance with a large number of parameters compared with the amount of case [30] due to a limited number of points per volume. It is, therefore, necessary to decrease the number of parameters by an algorithm that finds the best discrimination combination of parameters. We have applied the 'sequential floating forward selection' that first finds the most discriminative parameter based on the recognition score and, starting from that point, sequentially adds and deletes parameters until the highest possible recognition score is obtained [50] (Fig. 3). The findings were controlled by plotting dimensionality-performance graphs, where it could be seen that deterioration in classification occurred mostly after the addition of 15 parameters.

Univariate analysis

Analysis of variance (ANOVA) was used to compare performance of individual parameters in the comparison between the three types of tumours. Student's t-test was carried out to compare the series two-by-two. All statistical operations were carried out with Excel-software (Microsoft, Redmond, WA, USA).

Experimental set-up

Prognosis was estimated for all tumours by dividing the group into classes with survival: (1) =(mean survival minus standard deviation [SD]); (2) between (mean survival minus SD) and (mean survival plus SD) and (3) =mean survival plus SD. Following this rule, we divided colon carcinomas in survival classes =9 months, between 9 and 36 months and =36 months. MM-cases were divided in survival =2 months, between 2 and 9 months and =9 months. Patients with cervical carcinoma were divided into groups with survival =20 months, between 20 and 48 months and =48 months.

Table 2 – KNN classification of the prognosis in colorectal carcinoma

KNN selected parameters			*P* value ANOVA
V7			0.07
M5			0.15
G12			0.17
VES_CNT			0.18
V1			0.2
M6			0.2
V4			0.29
G1			0.65
G7			0.66
G9			0.82
G10			0.83
FD_G			0.92
	Confusion matrix (%)		
	1	2	3
1	–	25	75
2	6.3	50	43.8
3	3.2	6.5	90.3
Correctly classified cases using all parameters			70.6%
Correctly classified cases using IMD			56.9% (ANOVA: 0.2)
Correctly classified cases using fractal dimension			56.9% (ANOVA: 0.2)

Classes: (1) survival time <9 months; (2) between 9.1 and 22.4 months; and (3) >22.4 months. IMD, intratumoural micro-vessel density.

Results

Prognosis of Colorectal Carcinoma

Results of the prognosis of colorectal carcinoma with KNN and ANOVA are summarised in Table 2. Using the KNN-classifier, we obtained a general recognition score of 70.6% by a panel of 12 parameters, of which 11 were SSA-derived. Those relate to intervascular distances (total length of Gabriel's graph, number of vessels or reference area), to neighbourhood relationships (mean number of branches or node and fractal dimension of Gabriel's graph) and to distribution characteristics (for Gabriel's graph: standard deviation [SD] distance to the nearest neighbours, skewness and kurtosis of the number of branches or node, for minimum spanning tree: skewness and kurtosis of the length of the branches and for Voronoi diagram: SD of polygon shape and skewness of polygon area). The twelfth selected parameter is the IMD obtained with image analysis (VES_CNT). The recognition scores obtained

Table 3 – KNN classification of the prognosis of malignant mesothelioma

KNN selected parameters			*P* value ANOVA
M11			0.02
G3			0.02
PAPAREA			0.09
Age			0.09
M14			0.09
V1			0.11
VES_PERIM			0.21
V11			0.87
M10			0.99
	Confusion matrix (%)		
	1	2	3
1	–	100	–
2	–	91.7	8.3
3	–	11.1	88.9
Correctly classified cases using all parameters			86.4%
Correctly classified cases using IMD			60.9% (ANOVA: <0.001)
Correctly classified cases using fractal dimension			60.9% (ANOVA: 0.2)

Classes: survival 1: <2.6 months, 2: between 2.6 and 3: 9.2 months and >9.2 months.

Table 4 – KNN-classification of the prognosis of invasive cervical carcinoma

KNN selected parameters			*P* value ANOVA
VASCPERM			<0.001
G3			0.353735188
G11			0.38
V10			0.43
M14			0.95
	Confusion matrix (%)		
	1	2	3
1	85.7	–	14.3
2	9.1	81.8	14.3
3	–	16.7	83.3
Correctly classified cases using all parameters			83.3%
Correctly classified cases using IMD			25.0% (ANOVA: 0.4)
Correctly classified cases using fractal dimension			29.2% (ANOVA: 0.8)

Classes: 1: survival <20 months, 2: between 20 and 48 months and 3: >48 months.

solely with IMD or with the fractal dimension were much lower (56.9% and 29.2%, respectively). No parameter showed independent value with ANOVA-analysis ($P>0.05$), yet the SSA-parameters are ranked first. This indicates a stronger correlation of patients' outcome with vessel positioning (and especially with intervascular distances) than with vessel number. As no clinical parameter is selected, the correlation with patients' outcome is weak.

Classification of Malignant Mesothelioma

Recognition scores, confusion matrices and parametric panels in the prognosis of malignant mesothelioma are summarised in Table 3. Mesothelioma is characterised by a short survival time, making subdivision only possible in small time ranges (survival <2.6 months, between 2.6 and 9.2 months and >9.2 months). Yet, we obtained an excellent recognition score of 86.4%. This rate is slightly higher than obtained with histological or morphonuclear parameters pointing to a high prognostic potential for angiogenesis. Two parameters show individual statistical significance (mean of distance to nearest neighbours of minimum sparing tree and mean length of branches or references area of Gabriel's graph), and relate directly with intervascular distances. Other selected parameters are the age of the patient, mean vessel perimeter, immunostained area, number of vessels or reference area and SSA-histogram-derived parameters (kurtosis of number of branches or node of minimum sparing tree, kurtosis of distance to the nearest neighbour of minimum sparing tree and the SD of polygon form of Voronoi diagram are selected). The IMD is not selected, although ANOVA analysis showed a high individual discriminative value. Classification using the fractal dimension of the gray level image is similar to that obtained with IMD.

Note also that in the multivariate classification, IMDs obtained with image analysis (VES_CNT) are favoured over the manually assessed IMD (MAN_CNT). This indicates a higher prognostic relevance and confirms the data of Kumar-Singh *et al.* [39], who speculated that image filtering removes background staining, which could inadvertently be included in a manual assessment. We were able to obtain a large degree of automation in the quantitative assessment without the need for correction of the binary images, as long as the counter stain was very light. Therefore, we found the use of image analysis less laborious and suitable for a diagnostic pathology service.

Classification of Cervical Carcinoma

Recognition scores, confusion matrices and selected parameters in the prognosis of cervical carcinoma are summarised in Table 4. The highest recognition score that we obtained yielded 83.3%, with almost all parameters (except vascular permeation) being SSA-features. The mean length of branches and mean distance to the nearest neighbours of Gabriel's graph are most discriminative, pointing to different intervascular distances. The kurtosis of distance to the nearest neighbours of minimum sparing tree and mean of forms of Voronoi's are also selected, and point to differences in vessel arrangement. The fractal dimension also did not emerge as a potent prognosticator (recognition score 29.2%). The vascular permeation was most discriminative, and is the only parameter with independent prognostic value. These results confirm previously

reported data showing that the vascular permeation was most discriminative compared with other clinical parameters or IMD [40]. However, in the study by Tjalma *et al*. [40], the IMD had an independent discriminative value, whereas we only found a poor recognition score (25%) with the KNN-classifier using this feature.

Discussion

Tumour angiogenesis quantification can be regarded as a valuable prognostic tool in many tumours. Yet, most reports are based on mere counting (expressed as IMD), and do not take into account the spatial arrangement of the vessels, although the vascular pattern of the hot-spot may reflect a more complex angiogenic situation that is dependent on circulating factors, initial vascular structure and histological configuration [51,52]. The hypothesis of increasing the accuracy of predicting patients' outcome based on evaluation of vascular arrangement (quantified by the fractal dimension and syntactic structure parameters) rather than on IMD, was tested in this study.

We have examined the parametric performance in three different cancers. The first tumour, malignant mesothelioma, is aggressive (mean survival time: 6.6 months) characterised by a high IMD [39]. The second, colorectal carcinoma, has a longer survival (mean in this study: 22.4 months), with lower IMD [53], whereas the third, cervical carcinoma, has the best prognosis (mean: 34.3 months), although IMD is reported to be the highest [40]. The different degree of overall vascularisation is confirmed in our study and shows the relative value of IMD for prediction of patients' outcome. This may be explained as follows: Folkman *et al*. [54] has stated that, during tumour development, two distinct phenotypes can be noticed: (1) a prevascular dormant stage and (2) a vascular stage correlated with rapid tumour growth and a potential for metastasis. It can be hypothesised that the vascular situation in the dormant stage defines the starting situation at the time of angiogenic switch, and influences the degree of vascularisation in the initial active vascular phase. During further transformation, vascularisation will increase dependent upon various tumour-host interactions. Then, the relative increase in vascularisation is prognostically more important than the IMD, which reflects only the global vascularisation and might have serious limitations [55–57]. In this respect, it should be interesting to compare the vascularisation of a considerable number of normal pleural, colorectal and cervical tissues at different stages of the disease, using the vascularisation of the normal tissue as an internal standard for determining the degree of neo-angiogenesis in the tumour. It should be pointed out, however, that the rate of vascularisation is very difficult to measure over time because of the requirement of repeated biopsies or, alternatively, the poor resolution of available imaging techniques.

IMD calculation is usually based on counting blood vessels in so-called vascular 'hot-spots'. Those regions of intense vascularisation are biologically most important and comprise most relevant prognostic information in a rather small area. We concentrated our contextual analysis also on those hot spots to restrict the number of images, although some limitations were hereby introduced. The search for relevant hot spots requests an experienced observer who is familiar with the particular tumour histology and its angiogenic pattern, which made the process time-consuming and not entirely objective. Furthermore, as only a portion of the tumour is sectioned and analysed, not all hot spots are measured. To our knowledge, the spatial heterogeneity of the hot spots within one tumour has never been studied, but if there is such a spatial heterogeneity, measuring only certain hot spots might introduce a bias. In future designs, it could therefore be helpful to scan the whole tumour at low magnification with a motorised stage, mark the areas of intense staining and analyse them afterwards at higher magnification. This approach would allow a high degree of automation and will be more objective, making comparison of inter-laboratory data possible.

In this study, classification with a K-nearest neighbour classifier in three classes based only on IMDs, yielded recognition scores of 57%, 61% and 25% for malignant mesothelioma, colorectal carcinoma and invasive cervical carcinoma, respectively. Using the fractal dimension, we obtained similar results. These low values (especially for cervical carcinoma) indicate that prognosis is weakly correlated with vessel density or with general irregularity of the vascular pattern. This may seem contradictory to previous reports wherein IMD was found to be an independent prognosticator [39,40,53]. However, comparisons are hard to make as most studies are based on two class discriminations, using other classification systems with different class borders. Using all parameters, we found a stronger correlation with SSA-parameters than with IMD for all three cancers. The prognostic angiogenic correlation was weakest in cervical carcinoma, with only the vascular permeation having independent value. These data confirm the study of Tjalma *et al*. [40], wherein the vascular permeation was also found to be the best prognosticator. Contrarily, in colorectal carcinoma, SSA parameters were more discriminative than clinical data. None of the parameters showed independent value, but a combination yielded, recognition score of 71%, which is acceptable for clinical applications. The most discriminative parameters described differences in the statistical distribution of intervessel positioning (distance and IMD), indicating that survival time in colorectal carcinoma is inversely correlated with an increase in vessel number, arranged in a more irregular pattern. Lastly, in the analysis of mesothelioma, we found a high recognition score (86%) almost completely based on differences in angiogenic pattern. The two parameters with independent value (i.e. the mean distance to the

nearest neighbours of minimum spanning tree and the mean length of branches of the Gabriel's graph) describe intervascular distances and prove clearly the clinical usefulness of SSA.

By analysing these results, we might speculate that the relationship between prognosis and angiogenesis is stronger in aggressive neoplasms that cause death not by metastases but because the primary tumour is obstructing (e.g. malignant mesothelioma). As the malignant potential of obstructing tumours is dependent on the growth rate, which is limited by the vascular parameters, the survival is directly related to this degree of angiogenesis. Metastasising tumours, on the other hand, may cause death by secondary effects with a more vague relation to angiogenesis. This is, however, difficult to estimate, as reports on different types of tumours may have used varying methodology that makes the data impossible to compare. To allow a straightforward estimation of the importance of angiogenesis as a prognosticator in a particular tumour type, it is necessary to conduct studies that similarly analyse the angiogenic patterns of a variety of tumours, ranging form benign to highly malignant. Nevertheless, it can be concluded that, in all the investigated tumours, the intratumoural vascular network and its relation with prognosis is more correlated with contextual parameters than with IMD. Because it is impossible to study vascular function in this type of investigation, further studies are necessary to find out why this is so, but one can hypothesise that an optimal blood supply within the tumour is more controlled by the contextual organisation of the blood vessels than by the mere counts. The more accurate angiogenic description offered by SSA may be useful as an objective criterion for trials comparing different treatment modalities or for further exploitation as a prognosticator in a general diagnostic pathology service. Yet, because the methodology is rather labour intensive, further methodological investigation must be continued to increase the level of automation.

References

1 Folkman J. Wat is the evidence that tumors are angiogenesis dependent? *J Natl Cancer Inst* 1990;82:4–6.
2 Liotta LA, Kleiner MJ, Saidel GM. Quantitative relationships of intravascular tumor-cells, tumor vessels, and pulmonary metastases following tumor implantation. *Cancer Res* 1974; 34:997–1004.
3 Axelsson K, Ljung BME, Moore DH, *et al*. Tumor angiogenesis as a prognostic assay for invasive ductal breast-carcinoma. *J Natl Cancer Inst* 1995;87:997–1008.
4 Dickinson AJ, Fox SB, Persad RA, *et al*. Quantification of angiogenesis as an independent predictor of prognosis in invasive bladder carcinomas. *Br J Urol* 1994;74:762–766.
5 Gasparini G, Harris AL. Clinical importance of the determination of tumor angiogenesis in breast-carcinoma: much more than a new prognostic tool. *J Clin Oncol* 1995;13:765–782.
6 Maeda K, Chung YS, Takatsuka S, *et al*. Tumor angiogenesis and tumor-cell proliferation as prognostic indicators in gastric-carcinoma. *Br J Cancer* 1995;72:319–323.
7 Srivastava A, Laidler P, Davies RP, *et al*. The prognostic-significance of tumor vascularity in intermediate-thickness (0.76-4.0 Mm Thick) skin melanoma: a quantitative histologic study. *Am J Pathol* 1988;133:419–423.
8 Vermeulen PB, Verhoeven D, Hubens G, *et al*. Microvessel density, endothelial-cell proliferation and tumor-cell proliferation in human colorectal adenocarcinomas. *Ann Oncol* 1995;6:59–64.
9 Gasparini G, Bonoldi E, Viale G, *et al*. Prognostic and predictive value of tumour angiogenesis in ovarian carcinomas. *Int J Cancer* 1996;69:205–211.
10 Bevilacqua P, Barbareschi M, Verderio P, *et al*. Prognostic value of intratumoral microvessel density: a measure of tumor angiogenesis, in node-negative breast-carcinoma: results of a multiparametric study. *Breast Cancer Res Treat* 1995;36:205–217.
11 Khan AW, Dhillon AP, Hutchins R, *et al*. Prognostic significance of intratumoural microvessel density (IMD) in resected pancreatic and ampullary cancers to standard histopathological variables and survival. *Eur J Surg Oncol* 2002;28:637–644.
12 Gasinska A, Urbanski K, Adamczyk A, *et al*. Prognostic significance of intratumour microvessel density and haemoglobin level in carcinoma of the uterine cervix. *Acta Oncologica* 2002;41:437–443.
13 Ikeda N, Adachi M, Taki T, *et al*. Prognostic significance of angiogenesis in human pancreatic cancer. *Br J Cancer* 1999; 79:1553–1563.
14 Linder S, Blasjo M, von Rosen A, *et al*. Pattern of distribution and prognostic value of angiogenesis in pancreatic duct carcinoma: a semiquantitative immunohistochemical study of 45 patients. *Pancreas* 2001;22:240–247.
15 Leek RD. The prognostic role of angiogenesis in breast cancer. *Anticancer Res* 2001;21:4325–4331.
16 Arora R, Joshi K, Nijhawan R, *et al*. Angiogenesis as an independent prognostic indicator in node-negative breast cancer. *Anal Quant Cytol Histol* 2002;24:228–233.
17 Papamichael D. Prognostic role of angiogenesis in colorectal cancer. *Anticancer Res* 2001;21:4349–4353.
18 Rubio L, Burgos JS, Lopez-Guerrero JA, *et al*. Expression of p53 protein and tumor angiogenesis as prognostic factors in nasopharyngeal carcinoma patients. *Pathol Res Pract* 2002;198:97–102.
19 Davidson SE, Ngan R, Wilks DP, *et al*. A comparison of four methods for assessing tumor vascularity in carcinoma of the cervix. *Int J Oncol* 1994;5:639–645.
20 Fox SB, Leek RD, Weekes MP, *et al*. Quantitation and prognostic value of breast-cancer angiogenesis: comparison of microvessel density, chalkey count, and computer image-analysis. *J Pathol* 1995;177:275–283.
21 Weidner N. Current pathologic methods for measuring intratumoral microvessel density within breast carcinoma and other solid tumors. *Breast Cancer Res Treat* 1995;36:169–180.
22 Goddard JC, Sutton CD, Furness PN, *et al*. A computer image analysis system for microvessel density measurement in solid tumours. *Angiogenesis* 2002;5:15–20.
23 Wild R, Ramakrishnan S, Sedgewick J, *et al*. Quantitative assessment of angiogenesis and tumor vessel architecture by computer-assisted digital image analysis: Effects of VEGF-toxin conjugate on tumor microvessel density. *Microvasc Res* 2000;59:368–376.
24 Garrido T, Riese HH, Aracil M, *et al*. Endothelial-cell differentiation into capillary-like structures in response to tumor-cell conditioned medium: a modified chemotaxis chamber assay. *Br J Cancer* 1995;71:770–775.
25 Paku S, Paweletz N. First steps of tumor-related angiogenesis. *Lab Invest* 1991;65:334–346.
26 Cross SS. The application of fractal geometric analysis to microscopic images. *Micron* 1994;25:101–113.
27 Kirchner LM, Schmidt SP, Gruber BS. Quantitation of angiogenesis in the chick chorioallantoic membrane model using fractal analysis. *Microvasc Res* 1996;51:2–14.
28 Baish JW, Jain RK. Cancer, angiogenesis and fractals. *Nat Med* 1998;4:984–984.
29 Sabo E, Boltenko A, Sova Y, *et al*. Microscopic analysis and significance of vascular architectural complexity in renal cell carcinoma. *Clin Cancer Res* 2001;7:533–537.
30 Heymans O, Fissette J, Vico P, *et al*. Is fractal geometry useful in medicine and biomedical sciences? *Med Hypotheses* 2000; 54:360–366.

31 Rossitti S. Energetic and spatial constraints of arterial networks. *Arq Neuropsiquiatr* 1995;53:333–341.
32 Sandau K, Kurz H. Modeling of vascular growth-processes: a stochastic biophysical approach to embryonic angiogenesis. *J Microscopy Oxford* 1994;175:205–213.
33 Marcelpoil R, Usson Y. Methods for the study of cellular sociology: Voronoi diagrams and parametrization of the spatial relationships. *J Theor Biol* 1992;154:359–369.
34 Raymond E, Raphael M, Grimaud M, *et al*. Germinal center analysis with the tools of mathematical morphology on graphs. *Cytometry* 1993;14:848–861.
35 van Diest P, Kayser K, Meijer G, *et al*. Syntactic structure analysis. *Pathologica* 1995;7:255–262.
36 Boedefeld WM, Bland KI, Heslin MJ. Recent insights into angiogenesis, apoptosis, invasion, and metastasis in colorectal carcinoma. *Ann Surg Oncol* 2003;10:839–851.
37 Kakolyris SA, Kaklamanis LG, Koukourakis MJ, *et al*. Angiogenesis and p53 expression in the colorectal adenoma-carcinoma sequence. *Oncol Res* 2000;12:203–208.
38 Edwards JG, Cox G, Andi A, *et al*. Angiogenesis is an independent prognostic factor in malignant mesothelioma. *Br J Cancer* 2001; 85:863–868.
39 Kumar-Singh S, Vermeulen PB, Weyler J, *et al*. Evaluation of tumour angiogenesis as a prognostic marker in malignant mesothelioma. *J Pathol* 1997;182:211–216.
40 Tjalma W, Van Marck E, Weyler J, *et al*. Quantification and prognostic relevance of angiogenic parameters in invasive cervical cancer. *Br J Cancer* 1998;108:170–174.
41 Bremer GL, Tiebosch ATMG, van der Putten HWHM, *et al*. Tumor angiogenesis: an independent prognostic parameter in cervical cancer. *Am J Obstet Gynecol* 1996;174:126–131.
42 Tjalma WA, Weyler JJ, Bogers JJ, *et al*. The importance of biological factors (bcl-2, bax, p53, PCNA, MI, HPV and angiogenesis) in invasive cervical cancer. *Eur J Obstet Gynecol Reprod Biol* 2001;97:223–230.
43 Fujiwaki R, Hata K, Iida K, *et al*. Vascular endothelial growth factor expression in progression of cervical cancer: correlation with thymidine phosphorylase expression, angiogenesis, tumor cell proliferation, and apoptosis. *Anticancer Res* 2000;20:1317–1322.
44 Weidner N, Folkman J. Tumoral vascularity as a prognostic factor in cancer. In: De Vita V, ed. *Important advances in oncology*. Philadelphia: Lippincott-Raven, 1996:167–190.
45 Bartlett ML. Comparison of methods for measuring fractal dimension. *Austral Phys Eng Sci Med* 1991;14:146–152.
46 Cross SS. Fractals in pathology. *J Pathol* 1997;182:1–8.
47 Cross SS, Cotton DWK. The fractal dimension may be a useful morphometric discriminant in histopathology. *J Pathol* 1992; 166:409–411.
48 Losa GA, Nonnenmacher TF. Self similarity and fractal irregularity in pathologic tissues. *Mod Pathol* 1996;9:174–182.
49 Fukunaga K. *Introduction to statistical pattern recognition*. London: Academic Press, 1990.
50 Pudil P, Novovicova J, Kittler J. Floating search methods in feature selection. *Patt Rec Lett* 1994;15:1119–1125.
51 Byrne HM, Chaplain MAJ. Mathematical-models for tumor angiogenesis: numerical simulations and nonlinear-wave solutions. *Bull Math Biol* 1995;57:461–486.
52 Nekka F, Kyriacos S, Kerrigan C, *et al*. A model of growing vascular structures. *Bull Math Biol* 1996;58:409–424.
53 Vermeulen PB, Verhoeven D, Fierens H, *et al*. Microvessel quantification in primary colorectal-carcinoma: an immunohistochemical study. *Br J Cancer* 1995;71:340–343.
54 Folkman J, Watson K, Ingber D, *et al*. Induction of angiogenesis during the transition from hyperplasia to neoplasia. *Nature* 1989; 339:58–61.
55 Hansen S, Grabau DA, Bak M, *et al*. Tumour angiogenesis by vascular grading is of prognostic significance in breast cancer. *Eur J Cancer* 1998;34:S102–S102.
56 Vermeulen PB, Libura M, Libura J, *et al*. Influence of investigator experience and microscopic field size on microvessel density in node-negative breast carcinoma. *Breast Cancer Res Treat* 1997; 42:165–172.
57 Vermeulen PB, Nia PS, Colpaert C, *et al*. Lack of angiogenesis in lymph node metastases of carcinomas is growth pattern-dependent. *Histopathology* 2002;40:105–107.